Journal of Thermal Analysis and Calorimetry, Vol. 96 (2009) 1, 133–140

ELECTRICAL CONDUCTIVITY IN SOLID SOLUTIONS AND IN TWO-PHASE REGIONS OF THE SILVER HALIDE-BIVALENT METAL (CADMIUM, COBALT, ZINC) HALIDE SYSTEMS

Agata Górniak[*], *Alina Wojakowska, Stanisława Plińska and E. Krzyżak*

Wrocław Medical University, Department of Inorganic Chemistry, Laboratory of Thermal Analysis, ul. Szewska 38,
50139 Wrocław, Poland

Electrical conductivity of solid systems AgX–MX_2 (where *M*=Cd, Co, Zn and *X*=Cl, Br) were measured in a large range of temperature and compositions. Activation energies and conductivity values *vs*. composition are presented and discussed in relation to phase equilibria in the respective systems. Maximum of the conductivity value and stabilization of the activation energy have been found for silver halides doped heavily with divalent cation e.g. in the systems forming solid solutions on the silver halide side. Disorder in AgBr on the approach to melting, expected to be higher than in AgCl, has been shown by means of original DSC curves presented for both halides.

Keywords: *bivalent cations, ionic conductivity, phase diagrams, silver halides, solid-state*

Introduction

Solid silver halides: AgCl and especially AgBr reveal an extraordinary rise in electrical conductivity before melting, up to above 10 and 50 Ω^{-1} m^{-1} [1, 2], respectively. This effect was examined many times [3–7] and attributed mainly to an excessive increase of lattice defects concentration near the melting point [8–10]. It was also discussed in terms of premelting behavior [11, 12]. A much pronounced premelting effect in AgBr than in AgCl has been also observed on our DSC curves as indicated by a change of the slope of the baseline before melting (Fig. 1).

Electrical conductivity of ionic crystals may increase (or decrease) with addition of aliovalent ions, varying the defect concentration in the material. This was shown for the first time by Koch and Wagner [13] in AgCl and AgBr crystals doped with Cd^{2+} and Pb^{2+} halides. The problem was later frequently studied in view of understanding transport processes in these compounds [1–6, 8, 14–26]. The substitution of homovalent ions in solid solutions or two-phase mixtures [27, 28] as well as dispersions of electrically inert compounds [29, 30] may also lead to large changes in the ionic conductivity.

In amorphous materials, like ion-conducting silver phosphate glasses, high ionic conductivities has been also acquired by doping with divalent cations of transition metals: manganese [31], iron [31], cobalt [32], zinc [31, 33] and cadmium [32, 33]. Silver phosphate glasses doped with zinc and cadmium halides have been proposed to be used as electrolytes in solid-state batteries [34]. Silicate-phosphate glasses doped with K, Mg or Ca cations [35, 36] could be used as glassy fertilizers, in view of influence of doping on their biological activity.

In this work we present results of conductivity measurements, as a function of temperature and composition on solidified mixtures of AgCl or AgBr with respective chloride or bromide of bivalent metal:

$AgCl+CdCl_2$ [37]	$AgBr+CdBr_2$
$AgCl+CoCl_2$	$AgBr+CoBr_2$
$AgCl+ZnCl_2$	$AgBr+ZnBr_2$

A significant feature of the AgCl–$CdCl_2$ [38] and AgBr–$CdBr_2$ [39] phase equilibria is that very large ar-

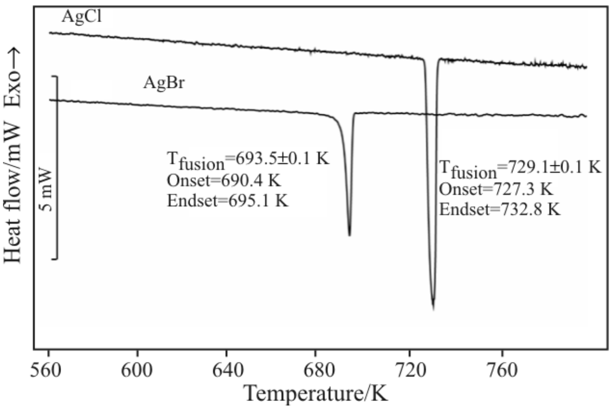

Fig. 1 Original DSC curves for AgCl and AgBr, obtained on heating at 1 K min^{-1}

---

[*] Author for correspondence: agata.gorniak@chnorg.am.wroc.pl

1388–6150/$20.00

Akadémiai Kiadó, Budapest, Hungary
Springer, Dordrecht, The Netherlands

eas of solid solutions based on the corresponding silver halide are formed, whilst phase diagrams involving cobalt(II) [40] and zinc halides [41] are of the eutectic type. Our results reveal the influence of doped cations on electrical behavior as well as confirm phase relations in the examined systems.

Experimental

Conductivity measurements as a function of temperature and composition were performed by AC technique. Capillary-type silica cells were used [42]. The measurements begun after the investigated mixture had melted under argon atmosphere, filled up the capillary and thus after an electrical contact between two platinum electrodes has been established. Several cycles of heating and cooling within a suitable temperature range were carried out. The heating or cooling rates did not exceed 1 K min^{-1}, which was controlled by an Eurotherm controller/programmer instrument type 818.

The conductances in the $AgBr–CdBr_2$ system were measured using a conductometer Taccusel CD 810 [43, 44]. The frequency dependence was checked in the range from 62.5 to 16000 Hz and was found to be negligible. Measurements were thus taken at 1000 Hz.

The conductances in the silver halide–cobalt halide systems and in the silver halide–zinc halide systems were measured using a conductometer CDM 230 Radiometer Analytical [45, 46]. The applied frequency of alternating current was set automatically from 94 to 46900 Hz, depending on the value of the resistance measured.

The temperature was measured with an accuracy of ±1 K by means of a Pt/PtRh thermocouple. Data acquisition and analysis were controlled with a computer, the software of which had been developed expressly for this type of investigation. Conductivity and temperature were simultaneously registered by the computer every 10 s.

Phase equilibria in the $AgX–MX_2$ systems (where X=Cl or Br and M=Cd, Co or Zn) were studied beforehand [39–41] by differential scanning calorimetry (Mettler Toledo DSC25) complemented by X-ray diffraction method (DRON-type diffractometer) and conductivity measurements.

Mixtures under examination were prepared prior to measurements from anhydrous salts of high purity [37, 39, 41, 47]. Samples for DSC experiments were prepared directly in silica ampoules next sealed under vacuum [48-–50]. All handling of samples involving zinc halides was undertaken in a glovebox [41].

Results and discussion

Within regions of temperature where the dependence of the specific conductivity $\sigma/\Omega^{-1}\ \text{m}^{-1}$ on temperature T/K obeys the Arrhenius type equation: $\ln\sigma=\ln\sigma^0–E_a/RT$, respective pre-exponential factors, activation energies for conduction $E_a/\text{kJ mol}^{-1}$ and the standard deviation s of the function ln σ, calculated by the method of least squares, are gathered in Tables 1–5.

Conductivity isotherms and activation energies for conduction as well as phase diagrams of the corresponding systems are presented in Figs 2–6. Appropriate values of electrical conductivity and activation energy for the pure silver halides are taken from Abbink and Martin [16] (silver chloride) and Müller [3] (silver bromide).

$AgCl+CdCl_2$ and $AgBr+CdBr_2$

Phase diagrams of the systems $AgCl–CdCl_2$ [38] and $AgBr–CdBr_2$ [39] are quite similar. They are presented

Table 1 Parameters of Arrhenius formula $\ln\sigma=\ln\sigma^0–E_a/RT$ for solid mixtures $CdBr_2(1)+AgBr(2)$

X_{AgBr}	ΔT/K	$\ln(\sigma^0/\Omega^{-1}\ \text{m}^{-1})$	$\ln(s/\Omega^{-1}\ \text{m}^{-1})$	E_a/R/K	$E_a/\text{kJ mol}^{-1}$
0.020	581–725	5.1925	0.0133	5758.6	47.9±0.1
0.050	588–667	10.0060	0.0123	6095.3	50.7±0.1
0.070	580–680	8.5269	0.0208	6088.6	50.6±0.2
0.200	641–690	9.4735	0.0043	5512.0	45.8±0.1
0.400	633–694	9.5309	0.0063	4662.1	38.8±0.1
0.600	561–662	11.8040	0.0015	5464.3	45.4±0.1
0.750	610–675	9.4460	0.0016	3745.1	31.1±0.1
0.850	578–671	9.8721	0.0040	3875.7	32.2±0.1
0.920	645–667	11.1510	0.0011	4999.3	41.6±0.2
0.960	628–671	14.1500	0.0077	7113.5	59.1±0.1
1.000*	448–673				81.77

*according to [3], P. Müller, Phys. Stat. Solidi, 21 (1967) 693

Table 2 Parameters of Arrhenius formula $\ln\sigma=\ln\sigma^0-E_a/RT$ for solid mixtures $CoCl_2(1)+AgCl(2)$

X_{AgCl}	ΔT/K	$\ln(\sigma^0/\Omega^{-1}\,\mathrm{m}^{-1})$	$\ln(s/\Omega^{-1}\,\mathrm{m}^{-1})$	E_a/R/K	E_a/kJ mol^{-1}
0.150	530–640	15.0232	0.0642	10262.4	85.3±0.9
0.500	545–645	17.7126	0.1040	10868.6	90.4±1.9
0.600	585–640	17.2167	0.0562	10495.4	87.3±2.2
0.800	615–650	16.7057	0.0662	9683.3	80.5±6.9
0.900	580–660	17.2651	0.0764	9802.0	81.5±2.2
1.000*	425–645				76.31

*according to [16], H. C. Abbink and D. S. Martin, Jr., J. Phys. Chem. Solids, 27 (1966) 205

Table 3 Parameters of Arrhenius formula $\ln\sigma=\ln\sigma^0-E_a/RT$ for solid mixtures $CoBr_2(1)+AgBr(2)$

X_{AgBr}	ΔT/K	$\ln(\sigma^0/\Omega^{-1}\,\mathrm{m}^{-1})$	$\ln(s/\Omega^{-1}\,\mathrm{m}^{-1})$	E_a/R/K	E_a/kJ mol^{-1}
0.150	511–623	10.8890	0.0700	7430.0	61.8 ±0.6
0.300	515–617	15.3293	0.0473	9578.2	79.6 ±0.4
0.500	539–665	17.2441	0.0561	10559.3	87.8 ±0.5
0.600	550–610	17.8947	0.0428	11096.8	92.4 ±0.5
0.700	500–595	18.3831	0.0661	11074.3	92.1 ±0.5
0.830	525–620	18.8141	0.0300	1111.8	92.4 ±0.2
0.880	540–635	19.0010	0.0729	10543.4	87.7 ±0.1
0.930	540–620	19.5186	0.0277	10604.1	88.2 ±0.2
0.960	540–625	19.6499	0.0335	10648.5	88.5 ±0.3
1.000*	448–675				81.77

*according to [3], P. Müller, Phys. Stat. Solidi, 21 (1967) 693

Table 4 Parameters of Arrhenius formula $\ln\sigma=\ln\sigma^0-E_a/RT$ for solid mixtures $ZnCl_2(1)+AgCl(2)$

X_{AgCl}	ΔT/K	$\ln(\sigma^0/\Omega^{-1}\,\mathrm{m}^{-1})$	$\ln(s/\Omega^{-1}\,\mathrm{m}^{-1})$	E_a/R/K	E_a/kJ mol^{-1}
0.400	473–504	40.2599	0.0357	21782.7	181.1±0.7
0.500	470–490	31.2563	0.1641	17751.3	147.6±5.0
0.600	454–503	17.4763	0.0815	10875.3	90.4±0.86
0.800	454–500	19.6871	0.0930	11766.3	97.8 ±1.0
1.000*	425–526				73.59

*according to [16], H. C. Abbink and D. S. Martin, Jr., J. Phys. Chem. Solids, 27 (1966) 205

Table 5 Parameters of Arrhenius formula $\ln\sigma=\ln\sigma^0-E_a/RT$ for solid mixtures $ZnBr_2(1)+AgBr(2)$

X_{AgBr}	ΔT/K	$\ln(\sigma^0/\Omega^{-1}\,\mathrm{m}^{-1})$	$\ln(s/\Omega^{-1}\,\mathrm{m}^{-1})$	E_a/R/K	E_a/kJ mol^{-1}
0.200	498–526	24.1279	0.2337	14433.0	120.0±4.2
0.400	498–526	15.0051	0.1366	9897.9	82.3±3.6
0.600	498–531	22.4734	0.2257	13363.8	111.1±1.8
0.800	454–520	17.9343	0.1601	10643.1	88.5±0.6
1.000*	448–673				81.77

*according to [3], P. Müller, Phys. Stat. Solidi, 21 (1967) 693

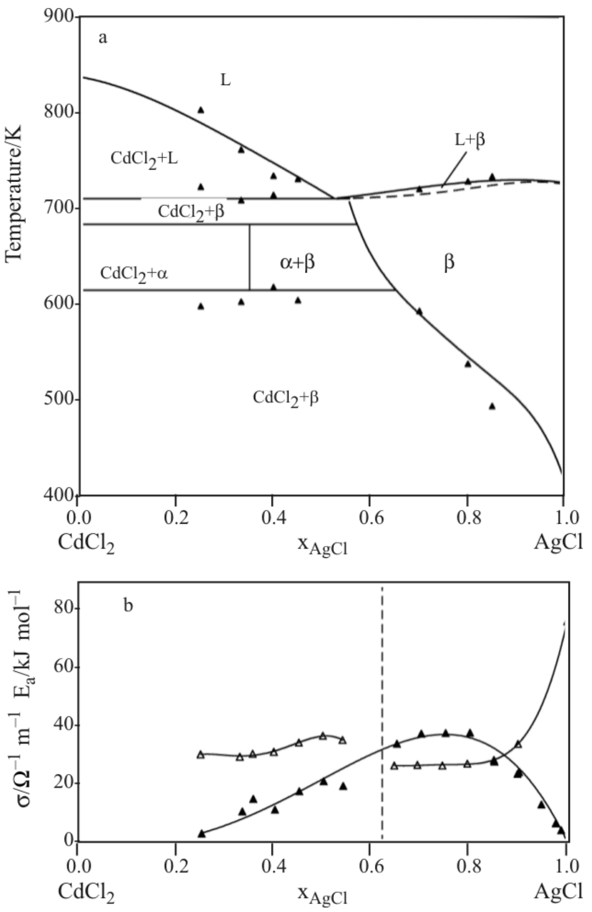

Fig. 2 a – Shape of the phase diagram of the AgCl–CdCl$_2$ system according to [38]; ▲ – conductivity measurements [37]; b – △ – activation energy for conduction and ▲ – conductivity isotherm at 623 K for the system AgCl–CdCl$_2$ (according to [37]). Vertical dotted line indicates the limit of the solid solution based on AgCl

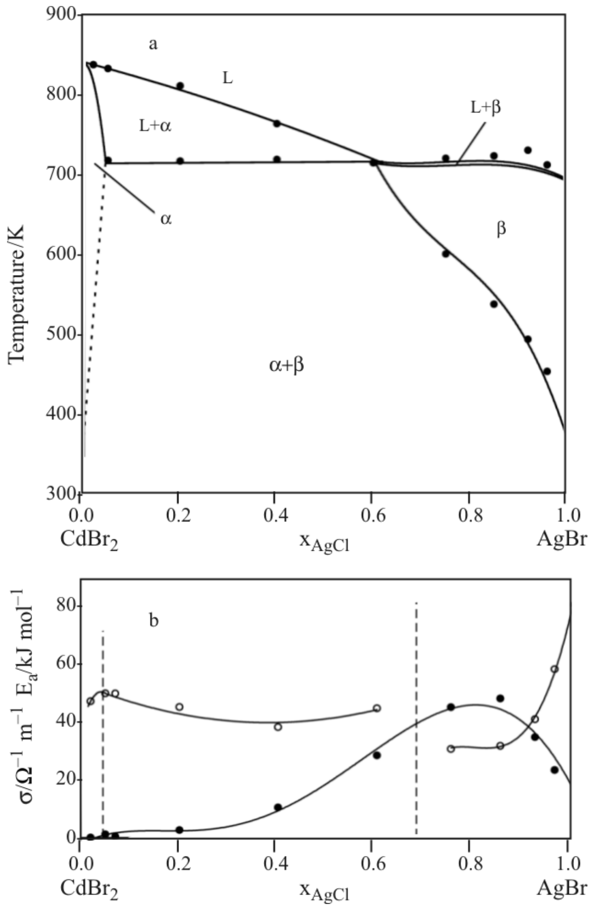

Fig. 3 a – Shape of the phase diagram of the AgBr–CdBr$_2$ system according to [39]; ● – conductivity measurements; b – ○ – activation energy for conduction and ● – conductivity isotherm at 648 K for the system AgBr–CdBr$_2$. Vertical dotted line indicates the limit of the solid solution based on AgBr

in Figs 2a and 3a, respectively. Complementary data on phase transitions, obtained in the course of our electrical conductivity measurements are included as well.

Main features of phase equilibria in the AgCl–CdCl$_2$ and AgBr–CdBr$_2$ systems are:

- very large areas of solid solutions based on the corresponding silver halide, extending to as far as 40 mol% cadmium dihalide
- very small areas between liquidus and solidus corresponding to deposition of this solid solution

The borders between solid solutions based on silver halides and the two-phase solid-state regions have been confirmed by our measurements of the electrical conductivity. A narrow solid solution (<4.5 mol% AgBr) is also formed on the CdBr$_2$ side (Fig. 3a). This limit was estimated with the help of conductivity measurements as well. The solid solubility in both systems falls while temperature is decreasing and becomes negligible below about 400 K.

Values of electrical conductivity at 623 and 648 K as well as activation energies for conduction for the systems AgCl–CdCl$_2$ and AgBr–CdBr$_2$ are plotted *vs.* composition in Figs 2b and 3b, respectively.

At temperatures of isotherms taken into consideration, solid solutions based on AgCl or AgBr show an important increase in conductivity with the concentration of Cd^{2+}, until around 20 mol% CdCl$_2$ or 15 mol% CdBr$_2$, respectively. At the maximum, the value of electrical conductivity in the AgCl+CdCl$_2$ solid solution is about 40 times higher than in pure AgCl and the value of electrical conductivity in the AgBr+CdBr$_2$ solid solution is about 3 times higher than in pure AgBr. Similarly, one can see from Fig. 7, that experimental values of the conductivity for the mixtures under investigation rich in AgBr, are higher than those for pure AgBr.

This increase of conduction may arise from the increase in the concentration of vacancies on the cationic sublattice due to addition of Cd^{2+}, a cation with higher valence than Ag$^+$. Electrical conductivity in the two-phase

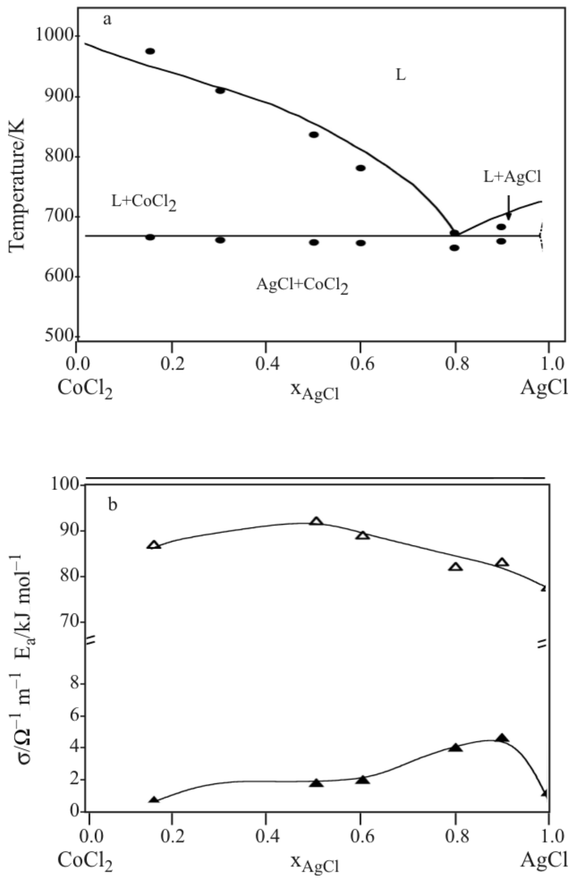

Fig. 4 a – Shape of the phase diagram of the AgCl–CoCl$_2$ system according to [40]; ● – conductivity measurements; b – △ – activation energy for conduction and ▲ – conductivity isotherm at 623 K for the system AgCl–CoCl$_2$

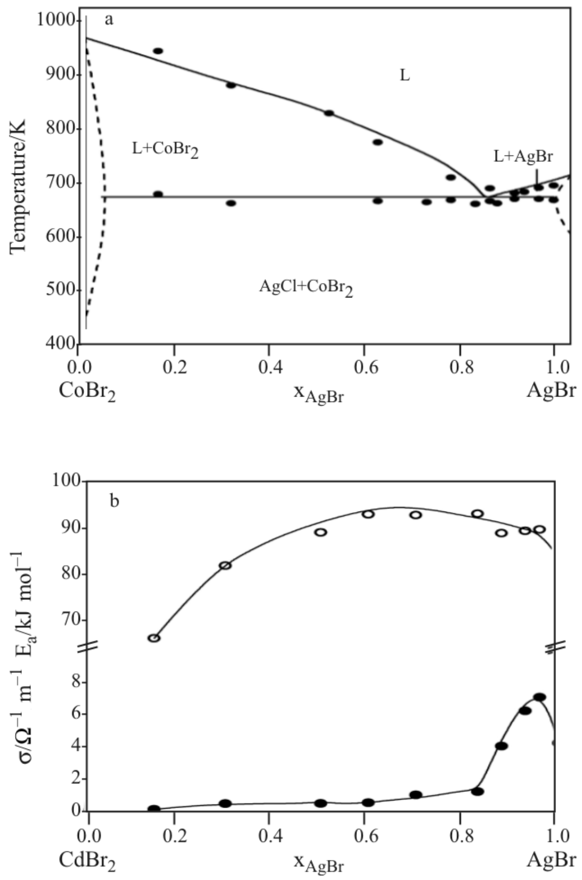

Fig. 5 a – Shape of the phase diagram of the AgBr–CoBr$_2$ system according to [40]; ● – conductivity measurements; b – ○ – activation energy for conduction and ● – conductivity isotherm at 600 K for the system AgBr–CoBr$_2$

solid-state regions (Figs 2a and 3a) is lower than in the solid solutions and decreases continuously with the concentration of cadmium dibromide.

An anomalous rise in electrical conductivity of AgCl and AgBr within 150 K of their melting temperatures results in an upwards curvature of the Arrhenius plots for these silver halides in the high temperature region [10, 22]. Our measurements of electrical conductivity show that the Arrhenius equation is valid for the whole temperature range of AgCl+CdCl$_2$ solid solutions [37], whilst the slope for AgBr+CdBr$_2$ solid solutions is not linear (Fig. 7). For this reason, activation energies in the AgBr–CdBr$_2$ system were calculated only for limited ranges of temperature (Table 1).

The activation energy for conduction in the solid AgCl (Fig. 2b) or AgBr (Fig. 3b) first falls rapidly, on account of doping with Cd^{2+} ions, but afterwards remains almost constant throughout the investigated composition range of the solid solution based on corresponding silver halide. Those values of activation energies in AgCl+CdCl$_2$ and AgBr+CdBr$_2$ solid solutions are very close to these of activation enthalpies for vacancy migration ΔH_v/kJ mol^{-1} [4] in the pure AgCl or AgBr, respectively:

	E_a/kJ mol^{-1}	ΔH_v/kJ mol^{-1}
AgCl	26.25±0.30	26.5±0.1
AgBr	31.14±0.20	31.3±0.1

This suggests that the vacancy mechanism of ionic conductivity is valid in AgCl+CdCl$_2$ and AgBr+CdBr$_2$ solid solutions, even relatively rich in the respective cadmium halide.

Average value of about 50 kJ mol^{-1} for the activation energy in the two-phase AgBr–CdBr$_2$ system is not far from a value of 53 kJ mol^{-1} obtained by Hanlon [14] for the activation enthalpy for diffusion in the heavily doped (3.30 atomic% Cd) sample.

AgCl+CoCl$_2$ and AgBr+CoBr$_2$

Phase diagrams involving cobalt(II) chloride and cobalt(II) bromide are of the simple eutectic type (Figs 4a and 5a). However, narrow limiting solid solutions, can be expected, especially in the bromide system.

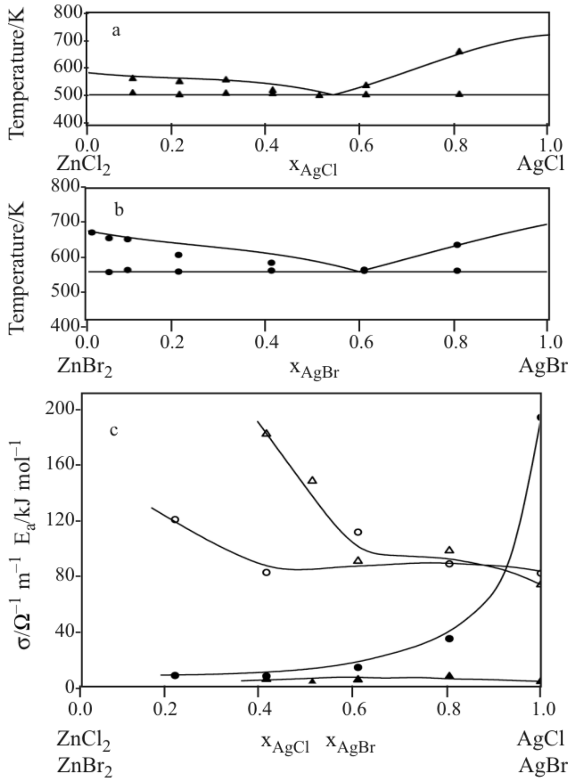

Fig. 6 a – Shape of the phase diagram of the AgCl–$ZnCl_2$ system according to [41]; ▲ – conductivity measurements; b – shape of the phase diagram of the AgBr–$ZnBr_2$ system according to [41]; ● – conductivity measurements; c – conductivity isotherms: ▲ – for AgCl–$ZnCl_2$ at 480, ● – for AgBr–$ZnBr_2$ at 500 K, as well as activation energy for conduction: △ – for AgCl–$ZnCl_2$ and ○ – AgBr–$ZnBr_2$

Concentration of the solute does not exceed 4 mol% on the AgBr side and 2.5 mol% of the $CoBr_2$ side.

Values of electrical conductivity at 623 and 600 K as well as activation energies for conduction for the systems AgCl–$CoCl_2$ and AgBr–$CoBr_2$ are plotted *vs.* composition in Figs 4b and 5b, respectively.

Initially, the conductivity rises with the cobalt(II) halide content in both systems. Beyond the eutectic composition a gentle decrease in the electric conductivity is observed. Contrary to silver halide–cadmium halide systems, activation energy for conduction in AgCl+$CoCl_2$ and AgBr+$CoBr_2$ mixtures is higher than in respective pure silver halides.

Samples of silver chloride and silver bromide doped with a very small concentration of Co^{2+} were studied as a function of temperature by tracer diffusity [25, 51, 52] and ionic conductivity measurements [26]. The activation energies for diffusion in the $CoCl_2$-AgCl and $CoBr_2$-AgBr systems have been determined to be 134 and 111 kJ mol^{-1} [25, 51], respectively. The data were interpreted in terms of a vacancy mechanism involving the migration of bound complexes of divalent cobalt with cation vacancies. Association enthalpies for Co^{2+} in AgCl and AgBr, being 26 and 19 kJ mol^{-1} [25, 26], respectively, were found to be lower in the bromide system.

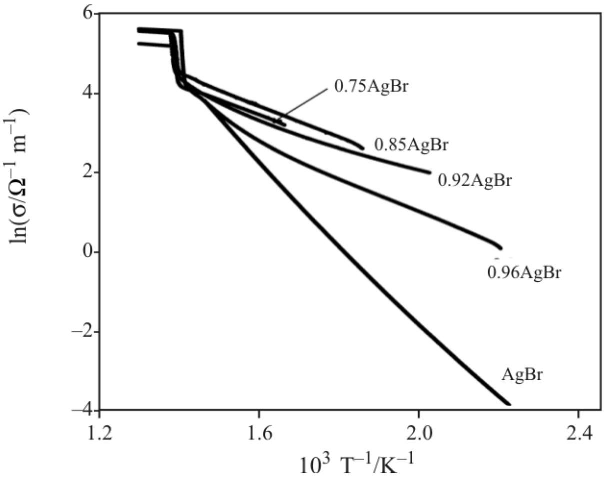

Fig. 7 Arrhenius plots for AgBr+$CdBr_2$ mixtures rich in AgBr [this work] and for pure AgBr [2]

AgCl+$ZnCl_2$ and AgBr+$ZnBr_2$

Phase diagrams of the AgCl–$ZnCl_2$ and AgBr–$ZnBr_2$ systems [41] are of the simple eutectic type (Figs 6a and b, respectively). Limiting solid solutions are negligible.

Values of electrical conductivity at 480 and 500 K as well as activation energies for conduction for the systems AgCl–$ZnCl_2$ and AgBr–$ZnBr_2$ are plotted *vs.* composition in Fig. 6c, respectively.

Electrical conductivity of AgCl does not change much in the two-phase area whilst that of AgBr, at the beginning higher about 40 times, falls down significantly on addition of zinc bromide. Finally they approach each other.

Values of activation energies for conduction for both systems are similar from the pure silver halide to around the respective eutectic point and then grow considerably.

It was found [18, 26] that the ion Zn^{2+} shows anomalous diffusion and ionic conductivity properties when doped into the silver halides e.g. an unusually large value of ion Zn^{2+}-vacancy binding energy in AgCl of the order of 60 kJ mol^{-1} [18], about twice as large as that for ion Cd^{2+}(28 kJ mol^{-1} [20]). This is thus the origin of its very high diffusity and rather low activation energy for diffusion in the $ZnCl_2$–AgCl system (74 kJ mol^{-1} [18]), taking place by means of vacancy mechanism [18].

It should be noted that correlations between transport properties and the electronic structure of the dopant ion, diffusing in silver halides, have been often researched. However, they are difficult to establish.

Thus in AgCl [51, 52], but not in AgBr [25], the activation energy for migration has shown a systematic change with increasing number of d-electrons for the first-row transition metal ions (V^{2+}, Cr^{2+}, Mn^{2+}, Fe^{2+}, Co^{2+}, Ni^{2+}). In contrast, for AgBr, but not for AgCl [26], a relationship between association enthalpy for divalent cation – vacancy complexes and the polarizability of the dopant ion has been found.

Conclusions

The systems AgCl–$CdCl_2$ and AgBr–$CdBr_2$, forming very large areas of solid solutions based on AgCl and AgBr, respectively, show an important increase in conductivity with the concentration of Cd^{2+} until around 15–20 mol% of the cadmium halide. Activation energy for conduction attains a saturation value within the respective solid solution.

In the systems AgCl–$CoCl_2$ and AgBr–$CoBr_2$, where solid solutions do not exceed 2–4 mol% of the cobaltous halide, a rise in conductivity is observed in these limits, followed by a sharp drop in the two-phase region.

The increase of conductivity on the silver halide side may arise from increase in the concentration of vacancies on the cationic sublattice due to addition of divalent cations.

Solid solutions in the systems AgCl–$ZnCl_2$ and AgBr–$ZnBr_2$ being negligible, the electric conductivity is little affected in the former whilst noticeably drops in the latter. Apparent different behavior of these systems can be explained the fact that AgBr reveals more ‘extra’ ionic conductivity than AgCl at temperatures chosen for presenting the respective conductivity isotherms.

References

1 I. Ebert and J. Teltow, Ann. Phys., 15 (1955) 268.
2 J. Teltow, Ann. Phys., 5 (1949) 63.
3 P. Müller, Phys. Status Solid., 21 (1967) 693.
4 J. K. Aboagye and R. J. Friauf, Phys. Rev. B, 11 (1975) 1654
5 A. P. Batra and L. M. Slifkin, J. Phys. Chem. Solids, 38 (1977) 687.
6 J. Corish and D. C. A. Mulcahy, J. Phys. C, 13 (1980) 6459.
7 D. A. Keen, W. Hayes and R. L. McGreevy, J. Phys.: Condens. Matter, 2 (1990) 2773.
8 P. Süptitz, Phys. Status Solid., 12 (1965) 555.
9 A. P. Batra and L. M. Slifkin, Phys. Rev. B, 12 (1975) 3473.
10 P. A. Varotsos and K. Alexopoulos, J. Phys. Chem. Solids, 39 (1978) 759.
11 D. A. Keen, V. M. Nield, R. L. McGreevy and W. Hayes, Physica B, 180–181 (1992) 798.
12 N. Hainovsky and J. Maier, Solid State Ionics, 76 (1995) 199.
13 E. Koch and C. Wagner, Z. Phys. Chem. B, 38 (1938) 295.
14 J. E. Hanlon, J. Chem. Phys., 32 (1960) 1492.
15 P. Müller, Phys. Status Solid., 12 (1965) 775.
16 H. C. Abbink and D. S. Martin, Jr., J. Phys. Chem. Solids, 27 (1966) 205.
17 A. L. Laskar, A. P. Batra and L. Slifkin, J. Phys. Chem. Solids, 30 (1969) 2061
18 A. P. Batra and L. M. Slifkin, Phys. Status Solid. (a), 19 (1973) 171.
19 H. G. Vomhof and J. Nölting, Ber. Bunsenges. Phys. Chem., 79 (1975) 991.
20 J. Corish and P. W. M. Jacobs, J. Phys. Chem. Solids, 33 (1972) 1799.
21 P. L. Lin and H. Schmalzried, Z. Phys. Chem. Neue Folge, 99 (1976) 161.
22 R. J. Friauf, J. Phys. (Paris), 38 (1977) 1077.
23 P. W. M. Jacobs, J. Corish and C. R. A. Catlow, J. Phys. C: Solid State Phys., 13 (1980) 1077.
24 B. A. Devlin and J. Corish, J. Phys. C: Solid State Phys., 20 (1987) 705.
25 E. F. Ekpo and A. P. Batra, J. Phys. Chem. Solids, 53 (1992) 1093.
26 R. J. Lieb and L. M. Slifkin, J. Phys. Chem. Solids, 57 (1996) 101.
27 K. Shahi and J. B. Wagner, Jr., J. Phys. Chem. Solids, 43 (1982) 713.
28 S. Hamakawa, M. Aniya and F. Shimojo, J. Therm. Anal. Cal., 81 (2005) 559.
29 C. C. Liang, J. Electrochem. Soc., 120 (1973) 1289.
30 A. Robledo, N. J. Garcia and J. C. Bazan, Solid State Ionics, 139 (2001) 303.
31 S. S. Das and V. Srivastava, J. Therm. Anal. Cal., 87 (2007) 363.
32 S. S. Das and P. Singh, J. Therm. Anal. Cal., 78 (2004) 731.
33 S. S. Das, B. P. Baranwal, P. Singh and V. Srivastava, Progr. Cryst. Growth Charact. Mater., 45 (2002) 89.
34 S. S. Das, B. P. Baranwal, C. P. Gupta and P. Singh, J. Power Sources, 114 (2003) 346.
35 I. Wacławska and M. Szumera, J. Therm. Anal. Cal., 84 (2006) 185.
36 M. Szumera and I. Wacławska, J. Therm. Anal. Cal., 88 (2007) 151.
37 A. Wojakowska, S. Plińska, J. Josiak and E. Kundys, High Temp. High Press., 30 (1998) 113.
38 R. Blachnik and J. E. Alberts, Z. Anorg. Allg. Chem., 489 (1982) 161.
39 A. Wojakowska, A. Górniak and A. Wojakowski, High Temp. High Press., 34 (2002) 349.
40 E. Krzyżak and A. Wojakowska, submitted to J. Therm. Anal. Cal., 93 (2008) 721.
41 A. Wojakowska, A. Górniak, A. Wojakowski and S. Plińska, J. Therm. Anal. Cal., 77 (2004) 41.
42 A. Wojakowska and E. Kundys, J. Mater. Sci., 25 (1990) 3780.
43 L. Rycerz, E. Ingier-Stocka, M. Cieślak-Golonka and M. Gaune-Escard, J. Therm. Anal. Cal., 72 (2003) 241.
44 B. Ziolek, L. Rycerz, S. Gadzuric, E. Ingier-Stocka and M. Gaune-Escard, Z. Naturforsch. (a), 60 (2005) 75.
45 A. Wojakowska and E. Krzyżak, Solid State Ionics, 176 (2005) 2711.

46 A. Wojakowska, S. Plińska and E. Krzyżak, J. Therm. Anal. Cal., 90 (2007) 355.

47 A. Wojakowska, E. Krzyżak and S. Plińska, J. Therm. Anal. Cal., 88 (2007) 525.

48 A. Wojakowska, E. Krzyżak and A. Wojakowski, J. Therm. Anal. Cal., 65 (2001) 491.

49 A. Wojakowska, E. Krzyżak and A. Wojakowski, Thermochim. Acta, 344 (2000) 55.

50 A. Wojakowska and E. Krzyżak, J. Therm. Anal. Cal., 83 (2006) 597.

51 A. P. Batra, J. P. Hernandez and L. M. Slifkin, Phys. Rev. Lett., 36 (1976) 876.

52 A. P. Batra, J. P. Hernandez and L. M. Slifkin, Phys. Rev. B, 22 (1980) 734.

Received: May 20, 2008
Accepted: June 26, 2008

DOI: 10.1007/s10973-008-9292-8